A Comparison Between Different Solutions for the Marchenko Multiple Eliminations Scheme

Rodrigo S. Santos[1*], Daniel E. Revelo[1], Reynam C. Pestana[2], Marcelo S. Souza[1], Victor Koehne[1], Diego F. Barrera[1,2], Jonathas Maciel[1]

[1]SENAI CIMATEC, Supercomputing Center; [2]INCT-GP/CNPq; Salvador, Bahia Brazil

Seismic reflection data can be used to generate high-resolution in-depth images capable of facilitating, with high precision, the correct positioning of wells in hydrocarbon exploration and production. However, images produced by migrating seismic data are often contaminated by artifacts due to multiple internal reflections. Different schemes can be used to avoid problems caused by these noises and to attenuate them, such as the Marchenko multiple elimination scheme (MME). Various solutions based on the MME method have been proposed in the literature. Therefore, in this work, we explore the MME based on the least-squares schemes (LSMME), the MME as Neumann series approximation solution (NMME), and the MME based on beyond Neumann method (BNMME), and compare them in terms of effectiveness and efficiency in different numerical examples.

Keywords: Multiple Reflections. MME. LSMME. NEMME. BNMME.

Introduction

Generating in-depth images is a common step in seismic data processing flows. In this step, seismic reflection data combined with the velocity and density fields of the medium is used to build an image of the subsurface. These images would be used to make geological interpretations and the best decisions to put new wells to explore or improve the O&G production. The seismic data, represented by the set of reflections experienced by waves in the subsurface structure in the source-receiver path, contains both primary and multiple reflections. However, to image the subsurface, standard imaging methods such as reverse time migration (RTM) are based on the single-scattering assumption, i.e., the recorded seismic data do not include waves that are reflected more than once in the subsurface before reaching the receivers. Although the internal multiples generally have lower energy than the primary reflections, the single-scattering assumption can lead to the generation of false events in the seismic images, resulting in mistakes in geologic interpretation, as shown by Santos and colleagues [1]. Zhang and colleagues [2] modified the projected Marchenko equations presented by Neut and Wapenaar [3] to introduce the method known as Marchenko multiple eliminations (MME), which is a data-driven algorithm capable of removing internal multiples of all orders without velocity information or adaptive filter. Later, Zhang and Slob [4] used a set of measured laboratory data to evaluate the performance of the MME. The same authors [5] showed the first example of applying the MME on a field data set from the Norwegian North Sea, which validated the capabilities of the MME schemes and showed that it could effectively eliminate internal multiples. Aiming to explore the potential of the MME approach, many techniques went on to be developed, such as the transmission-compensated Marchenko multiple eliminations (T-MME) derived by Zhang and colleagues [6], which is a scheme that eliminates multiple internal reflections and compensates for two-way transmission losses contained in primary reflections. Afterward, Zhang and Slob [7] developed a fast implementation of the MME scheme that reduces its computational cost by an order of magnitude. The MME solution proposed by Zhang and colleagues [2] is based on the

Received on 16 December 2022; revised 7 January 2023.
Address for correspondence: Rodrigo S. Santos. Rua da Mangueira, No 60, Pero Vaz, Salvador, Bahia, Brazil. Zipcode: 40.335-755. E-mail: rodrigo.santana@fieb.org.br.

J Bioeng. Tech. Health 2023;6(Suppl.1):17-22.

Neumann series approximation (NEMME), so recently, Santos and colleagues [1] have proposed to formulate the MME scheme as a least-squares problem (LSMME), which averts the convergence criterion of the Neumann series approximation, and evaluates this approach in a complex 2D synthetic numerical example. Subsequently, to reduce the MME empirical scale factor dependence, Santos and colleagues [8] proposed an alternative solution based on the beyond Neumann scheme (BNMME) and showed that BNMME is more suitable in situations where it is difficult to obtain an ideal scale factor. The experiments developed by Zhang and colleagues [2] and Santos and colleagues [1,8] showed that when seismic data have previously gone through a high-quality pre-processing stage, i.e., deghosting, removal of free-surface multiples, and deconvolution with an estimated source wavelet, the schemes NEMME, LSMME, and BNMME successfully eliminates or attenuates multiple internal reflections. However, despite the experiments showing the power of the referred schemes in attenuating the internal multiples, their computational performance still needs to be evaluated. In this paper, we focus on evaluating this computational performance when the effectiveness of attenuating noise remains constant by testing NEMME, LSMME, and BNMME using a simple and another complex model.

Theory

The schemes MME, LSMME, and BNMME are based on the projected Marchenko equations for the single-sided reflection response [8-10]:

$$\overline{\mathrm{U}}^{-}(\mathbf{x}_0'', \mathbf{x}_0', \mathrm{t}) = \left(\Theta_{\mathrm{t}_2-\epsilon}^{\infty}\mathbf{R}\overline{\delta} + \Theta_{\mathrm{t}_2-\epsilon}^{\infty}\mathbf{R}\overline{\mathrm{v}}_{\mathrm{m}}^{+}\right)(\mathbf{x}_0'', \mathbf{x}_0', \mathrm{t}), \tag{1}$$

$$\begin{cases} \overline{\mathrm{v}}_{\mathrm{m}}^{+}(\mathbf{x}_0', \mathbf{x}_0'', \mathrm{t}) = \left(\Theta_{\epsilon}^{\mathrm{t}_2-\epsilon}\mathbf{R}^{*}\overline{\mathrm{v}}^{\,-}\right)(\mathbf{x}_0', \mathbf{x}_0'', \mathrm{t}) \\ \overline{\mathrm{v}}^{-}(\mathbf{x}_0', \mathbf{x}_0'', \mathrm{t}) = \left(\Theta_{\epsilon}^{\mathrm{t}_2-\epsilon}\mathbf{R}\overline{\delta} + \Theta_{\epsilon}^{\mathrm{t}_2-\epsilon}\mathbf{R}\overline{\mathrm{v}}_{\mathrm{m}}^{+}\right)(\mathbf{x}_0', \mathbf{x}_0'', \mathrm{t})' \end{cases} \tag{2}$$

in which $\mathbf{x_i} = (\mathbf{x}_H, \mathbf{z_i})$ and $\mathbf{x}_H$ are the horizontal coordinates and $\mathbf{z_i}$ is the depth of an arbitrary boundary $\partial \boldsymbol{D}_i$, such that the acquisition surface $\partial \boldsymbol{D}_0$ will be defined by $\mathbf{x_0} = (\mathbf{x}_H, \mathbf{z_0})$ and t is the time. $\overline{\mathrm{U}}^{-}$ and $\overline{\mathrm{v}}^{\pm}$ represent the projected versions of the up-going Green's function and the down- and up-going focusing or filter function, respectively. The overline indicates that quantities have been convolved with the source wavelet. t_2 is the two-way travel time of the acquisition surface $\partial \boldsymbol{D}_0$ and a fictitious reflector at horizon $\partial \boldsymbol{D}_i$. The Θ is a truncation operator to exclude values outside the window $(\varepsilon, \mathrm{t} - \varepsilon)$, in which $\boldsymbol{\varepsilon}$ is a positive value to account for the finite bandwidth. $\boldsymbol{R}$ and $\boldsymbol{R^*}$ are multidimensional convolution and correlation operators [1,8]. Following Zhang and Slob [4], Equation (1) must be evaluated for each instant time t_2 and their value collected to be stored in a new function $\overline{\mathrm{R}}_{\mathrm{t}}$ containing only primary reflections as:

$$\overline{\mathrm{R}}_{\mathrm{t}}(\mathbf{x}_0'', \mathbf{x}_0', \mathrm{t} = \mathrm{t}_2) = \overline{\mathrm{U}}^{-}(\mathbf{x}_0'', \mathbf{x}_0', \mathrm{t}_2). \tag{3}$$

Neut and Wapenaar [3] showed that $\{\mathbf{R}\delta\}(\mathbf{x}_0'', \mathbf{x}_0', \mathrm{t})$ is equal to $\mathrm{R}(\mathbf{x}_0'', \mathbf{x}_0', \mathrm{t})$. From Equation (1), it is essential to note that to compute $\overline{\mathrm{U}}^{-}$, it is first necessary to obtain $\overline{\mathrm{v}}^{+}$.

<u>Neumann Series Solution</u>

As described by Santos and colleagues [1], if we organize the terms of Equation (2) and use the Neumann series expansion, we will obtain the following expression as a solution for Equation (2):

$$\overline{\mathrm{v}}_{\mathrm{m}}^{+}(\mathbf{x}_0', \mathbf{x}_0'', \mathrm{t}) = \left[\sum_{\mathrm{k}=1}^{\infty}\left(\Theta_{\epsilon}^{\mathrm{t}_2-\epsilon}\mathbf{R}^{*}\Theta_{\epsilon}^{\mathrm{t}_2-\epsilon}\mathbf{R}\right)^{\mathrm{k}}\overline{\delta}\right](\mathbf{x}_0', \mathbf{x}_0'', \mathrm{t}) \tag{4}$$

in which k represents the number of terms in the series that resemble the number of iterative iterations. The Marchenko multiple eliminations based on Equation (4) are conventionally named by the MME scheme. However, we must remember that the solution based on the Neumann series approximation converges only if

$$\left\|\Theta_{\epsilon}^{\mathrm{t}_2-\epsilon}\mathbf{R}^{*}\Theta_{\epsilon}^{\mathrm{t}_2-\epsilon}\mathbf{R}\right\| < 1 \tag{5}$$

LSMME

The LSMME approach treats the Marchenko multiple elimination problems as a linear system of the type $\mathbf{Ax} = \mathbf{b}$, where the solution $\mathbf{x}$ is the object of study. So, we can rewrite the down- and up-going filter functions of Equation (2) as the following linear system:

$$\begin{bmatrix} \mathbf{I} & -\Theta\mathbf{R} \\ -\Theta\mathbf{R}^* & \mathbf{I} \end{bmatrix} \begin{bmatrix} \bar{\mathbf{v}}^- \\ \bar{\mathbf{v}}_m^+ \end{bmatrix} = \begin{bmatrix} \Theta\bar{\mathbf{R}} \\ 0 \end{bmatrix} \tag{6}$$

The LSMME method obtains a solution for Equation (6) by formulating it as a least-squares problem (LS) and minimizing the sum of the squared residuals. To solve the linear system, we followed the approach implemented by Santos and colleagues [1] and applied the iterative method of Paige and Saunders, [11], which is based on a stable process.

BNMME

The BNMME scheme is based on solving the linear system in Equation (6) using the beyond Neumann method [12]. In this approach, the solution is obtained using the following recursive scheme:

$$\mathbf{x}_n = \sum_{k=0}^{n} (\mathbf{I} - \alpha_k \mathbf{A})^k \alpha_k \mathbf{b}, \tag{7}$$

in which α_k represents a relaxation parameter, which is updated according to

$$\alpha_k = \frac{\mathbf{r}_{k-1}^H \mathbf{A} \mathbf{r}_{k-1}}{\mathbf{r}_{k-1}^H \mathbf{A}^H \mathbf{r}_{k-1}} \tag{8}$$

with

$$\mathbf{r}_k = (\mathbf{I} - \alpha_{k-1}\mathbf{A})\mathbf{r}_{k-1}. \tag{9}$$

Materials and Methods

In order to check the presented Marchenko multiple elimination schemes, we compared them in two numerical experiments. The objective was to evaluate the schemes in qualitative and quantitative terms in the multiple reflections attenuation process. Thus, we fixed the computational and experimental architecture for each experiment.

We first generated the acoustic impulse reflection response R with a finite-difference time-domain modeling code. We were involved with a Ricker wavelet with a 20 Hz central frequency to represent seismic data ($\bar{R}$). The R and $\bar{R}$ terms are used as input to the schemes, and the output seismic data $\bar{R}_t$ contains only primary seismic reflections.

Results and Discussion

To evaluate the results, we chose the central shot gather (red star in Figures 1a, 1b, and 2a) for visualization of the effect of the multiple before and after the method application. In each situation, we compare the zero-offset trace to check if the phases and amplitudes of primary events were preserved.

Flat Layer Model

The first numerical example used is the flat layer model represented by the acoustic velocity and density values shown in Figures 1a and 1b, respectively. For this example, we have computed the reflection responses with 901 sources excited one by one and a fixed-spread array of 901 receivers with a spacing of 5 m located at the top of the model between -2.5 km and 2.5 km. The duration of each shot record is 4.0 s with a time sampling of 4 ms. In this experiment, 30 iterations were used for each scheme. Figure 1c shows the modeled synthetic data with labeled internal multiples interpretation (blue arrows). Figures 1d, 1e, and 1f show the output of NEMME, LSMME, and BNMME solutions, respectively, in which we observe that the events associated with multiple internal

Figure 1. (a) The velocity and (b) density values for the four-layer model with the red star indicates the shot position. The modeled reflection response in (c) and the retrieved data set using NEMME, LSMME, and BNMME, in (d), (e), and (f) respectively. The lines indicate the zero-offset traces selected to plot in Figure 1(g).

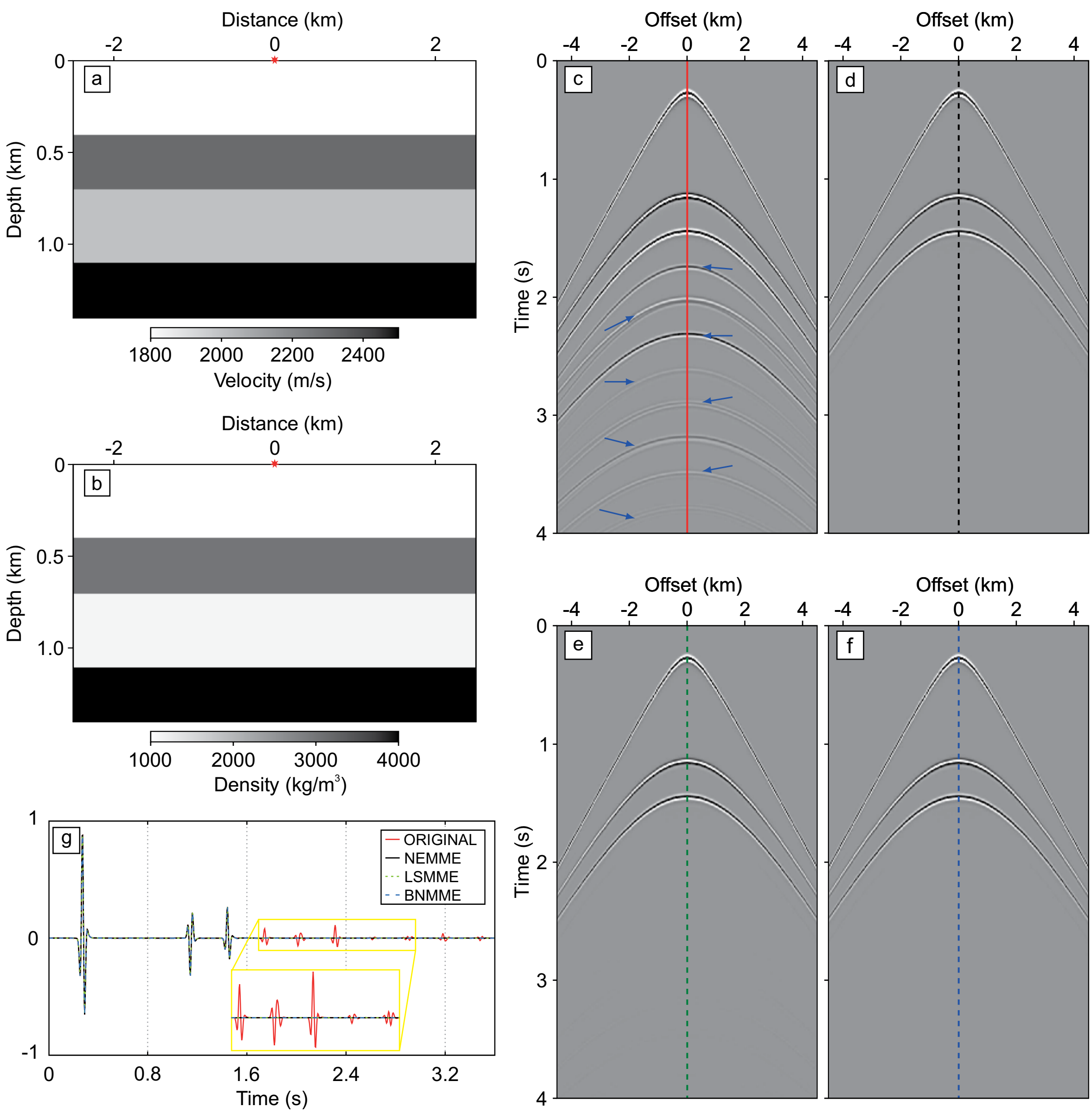

reflections signaled in Figure 1a were correctly attenuated. The dashed or solid lines in these figures indicate the selected zero-offset trace for analysis of the phases and amplitudes of the event. Figure 1g compares the zero-offset traces obtained by the three schemes, where we can see that the noise events were attenuated, preserving the amplitude and phase of the primary reflections. Figure 3 shows the computational cost for each scheme, having maintained a fixed computational structure to perform the experiments.

<u>Santos Basin Model</u>

The acoustic velocity model (Figure 2a) is named Santos basin model and simulates a realistic

Figure 2. (a) The velocity values for the Santos model where the red star indicates the shot position of a seismic source. The modeled reflection response in (a) and the retrieved data set using NEMME, LSMME, and BNMME, in (c), (d), and (e) respectively. The lines indicate the zero-offset traces selected to plot in Figure 2(f).

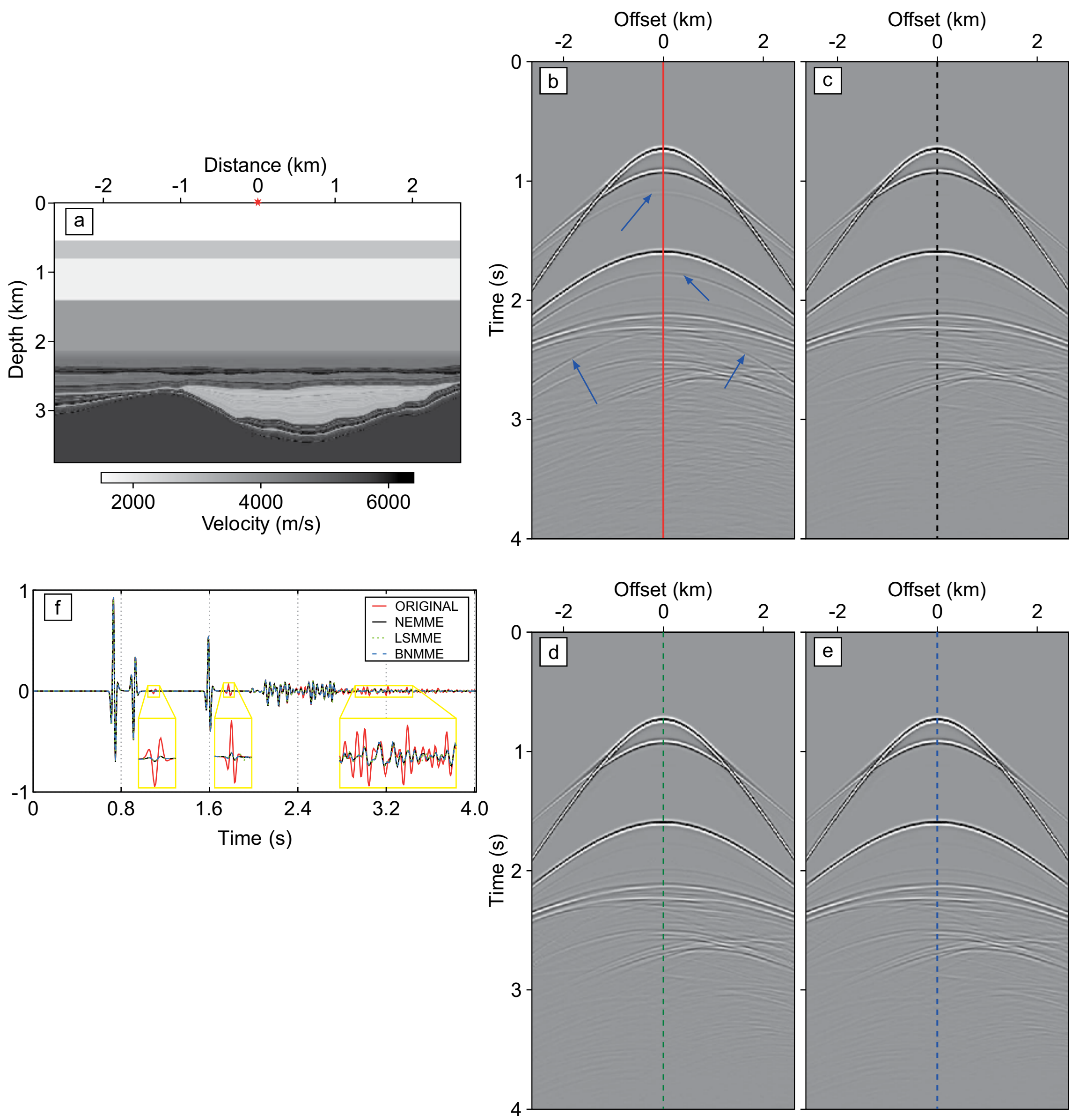

geological situation similar to those found in the sedimentary basins of the Brazilian continental shelf. For this numerical example, we computed the reflection responses with 526 sources excited one by one and a fixed-spread array of 526 receivers with a spacing of 10 m located at the model top between -2.625 km and 2.625 km. The duration of each shot record is 4.0 s with a sampling of 4 ms.

In this experiment, we used 10 iterations for each scheme. Figure 2b shows the modeled synthetic data with labeled internal multiples interpretation (blue arrows), and Figures 2c, 2d, and 2e show the output of NEMME, LSMME, and BNMME solutions, respectively. The dashed or solid lines in the figures indicate the zero-offset traces selected to plot in Figure 2f. By analyzing the shot gathers of Figures 2d, 2e, and 2f and the plot of the zero-offset traces of Figure 2f, we observe that the events associated with the multiple internal reflections were correctly attenuated, similar to what happened in the previous experiment.

The computational time spent on each scheme is also shown in Figure 3.

Conclusion

This study compared the NEMME, LSMME, and BNMME approaches to treat multiple internal reflections. The presented results showed that such schemes successfully attenuate these coherent noises as long as the data is submitted to a quality pre-processing. When the results are compared, these methods have similar effectiveness in noise attenuation. By analyzing the computational cost of the three methods, we observed that NEMME and BNMME have similar efficiency, but they have shown better performance than the LSMME. These results can be used as a decision approach for choosing multiple treatment methods.

Acknowledgments

We thank the editors and reviewers for their constructive comments and suggestions. CENPES/ Petrobras and ANP supported this work through the Marchenko project at SENAI CIMATEC We want to thank FINEP for the support of the Supercomputing Center of SENAI CIMATEC.

References

1. Santos RS, Revelo DE, Pestana RC, KoehneV, Barrera DF, Souza MS, Silva A. An application of the Marchenko internal multiple elimination scheme formulated as a least-squares problem. Geophysics 2021;86(5):1–70.
2. Zhang L, Slob E, van der Neut J, Wapenaar K. Artifact-free reverse time migration. Geophysics 2018;83(5):A65–A68.
3. van der Neut J, Wapenaar K. Adaptive overburden elimination with the multidimensional Marchenko equation. Geophysics 2016;81(5):T265–T284.
4. Zhang L, Slob E. Free-surface and multiple internal eliminations in one step without adaptive subtraction. Geophysics 2019;84(1):A7–A11.
5. Zhang L, Slob E. Marchenko multiple eliminations of a laboratory example. Geophysical Journal International 2020;221(2):1138–1144.

Figure 3. Normalized time consumed to perform the NEMME, LSMME, and BNMME schemes in the flat layer and Santos basin models.

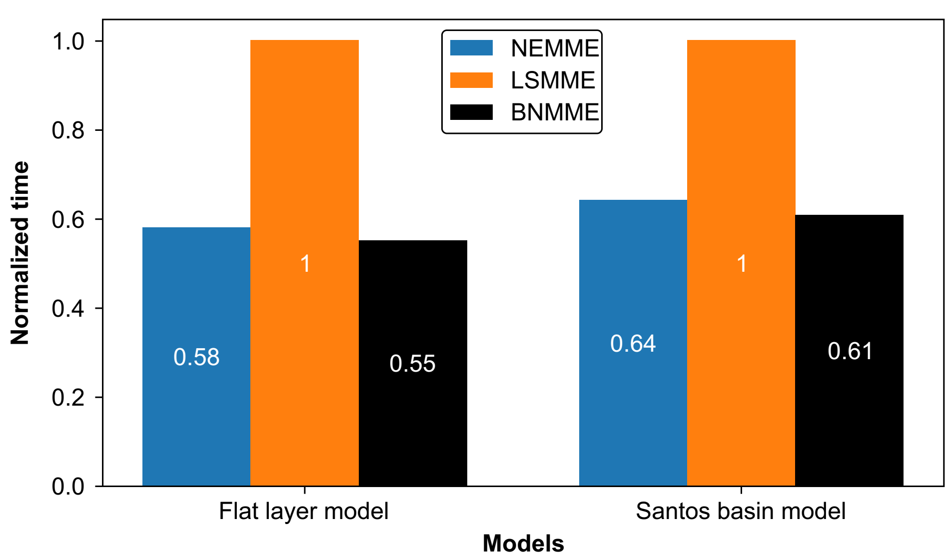

6. Zhang L, Thorbecke J, Wapenaar K, Slob E. Transmission compensated primary reflection retrieval in the data domain and consequences for imaging. Geophysics 2019;84(4):Q27–Q36.
7. Zhang L, Slob E. A fast algorithm for multiple elimination and transmission compensation in direct reflections. Geophysical Journal International 2020;221(1):371–377.
8. Santos R, Maciel J, Pestana R, Souza M, Koehne V, Revelo D, Barrera D, Paula R. A Marchenko multiple elimination solutions based on the beyond Neumann method. In: 83rd EAGE Annual Conference & Exhibition. European Association of Geoscientists & Engineers 2022:pp. 1–5.
9. Zhang L, Staring M. Marchenko scheme based internal multiple reflection elimination in acoustic wavefield. Journal of Applied Geophysics 2018;159:429–433.
10. Santos RS, Revelo DE, Pestana RC, Koehne V, Barrera DF, Souza MS. A least-squares based approach for the Marchenko internal multiple elimination scheme. In: SEG Technical Program Expanded Abstracts. Society of Exploration Geophysicists 2020:3184–3188.
11. Paige C, Saunders M. Algorithm 583. LSQR: Sparse linear equations and least squares problems. ACM Transactions on Mathematical Software 1982;8(2):195–209.
12. Maciel J, Pestana R, Barreira D. Stable solutions in Marchenko iterative scheme with beyond neumann. In: 82nd EAGE Annual Conference & Exhibition. European Association of Geoscientists & Engineers 2021:1–5.